Oncogene
https://doi.org/10.1038/s41388-017-0090-2

ARTICLE

TBX3 promotes proliferation of papillary thyroid carcinoma cells through facilitating PRC2-mediated p57^{KIP2} repression

Xiaomeng Li[1] · Xianhui Ruan[2] · Peitao Zhang[1] · Yang Yu[2] · Ming Gao[2] · Shukai Yuan[1] · Zewei Zhao[1] · Jie Yang[1] · Li Zhao[1]

Received: 25 June 2017 / Revised: 1 November 2017 / Accepted: 24 November 2017

Abstract

The T-box transcription factor TBX3 has been implicated in the patterning and differentiation of a number of tissues during embryonic development, and is overexpressed in a variety of cancers; however, the precise function of TBX3 in papillary thyroid carcinoma (PTC) development remains to be determined. In the current study, we report downregulation of TBX3 in PTC cells delays the G1/S-phase transition, decreases cell growth in vitro, and inhibits tumor formation in vivo. We identified p57^{KIP2} as a novel downstream target that serves as the key mediator of TBX3's control over PTC cell proliferation. Reduced expression of TBX3 resulted in increased p57^{KIP2} level, while knockdown of p57^{KIP2} rescues the cell-cycle arrest phenotype. In clinical PTC specimens, the expression of TBX3 is markedly upregulated and significantly correlated with advanced tumor grade, but negatively correlated with the expression of p57^{KIP2}. Mechanism investigation revealed that TBX3 directly binds to the *CDKN1C* gene promoter region, the coding gene of p57^{KIP2}, and represses its transcription. Furthermore, recruitment of main components of the PRC2 complex as well as class I histone deacetylases, HDAC1 and HDAC2, is required for TBX3 to fulfill the transcriptional repression function. Our findings illustrate the previously unknown function and mechanism in cell proliferation regulation by the TBX3-p57^{KIP2} axis and provide evidence for the contribution of the PRC2 complex and HDAC1/2. Targeting of this pathway may present a novel and molecular defined strategy against PTC development.

Introduction

T-box3 (TBX3), as a member of the T-box transcription factor family, plays a crucial role in embryonic development and also impacts on tumorigenesis. TBX3 is required for the development of the heart, limbs, mammary glands, and central nervous system [1–3]. Therefore, haploinsufficiency of the human *TBX3* gene results in ulnar-mammary syndrome characterized by hypoplasia of these structures [1]. During the past decade, a growing list of studies have reported deregulated levels of TBX3 in different types of cancers including breast, cervix, ovary, pancreas, liver cancers, and melanomas, where it plays a tumor promoter role [4–8]. TBX3 has been involved in several oncogenic processes, including proliferation, migration, and invasion [9–11]. Through repressing tumor suppressor p14^{ARF}/p19^{ARF}, cyclin-dependent kinase (CDK) inhibitor, p21^{WAF1}/^{CIP1}, TBX3 interferes with p53 dependent and independent apoptosis pathway and leads to increased proliferation and immortalization [12–15]. TBX3 was also found to enhance the anti-apoptotic ability of head and neck squamous cancer

Xiaomeng Li and Xianhui Ruan contributed equally to this work.

Electronic supplementary material The online version of this article (https://doi.org/10.1038/s41388-017-0090-2) contains supplementary material, which is available to authorized users.

✉ Jie Yang
yangj@tijmu.edu.cn

✉ Li Zhao
shzhaoli@tijmu.edu.cn

[1] Department of Biochemistry and Molecular Biology, School of Basic Medical Sciences, Tianjin Medical University, Tianjin 300070, China

[2] Department of Thyroid and Neck Tumor, Tianjin Medical University Cancer Institute and Hospital, National Clinical Research Center for Cancer, Key Laboratory of Cancer Prevention and Therapy, Tianjin 300060, China

Published online: 07 March 2018

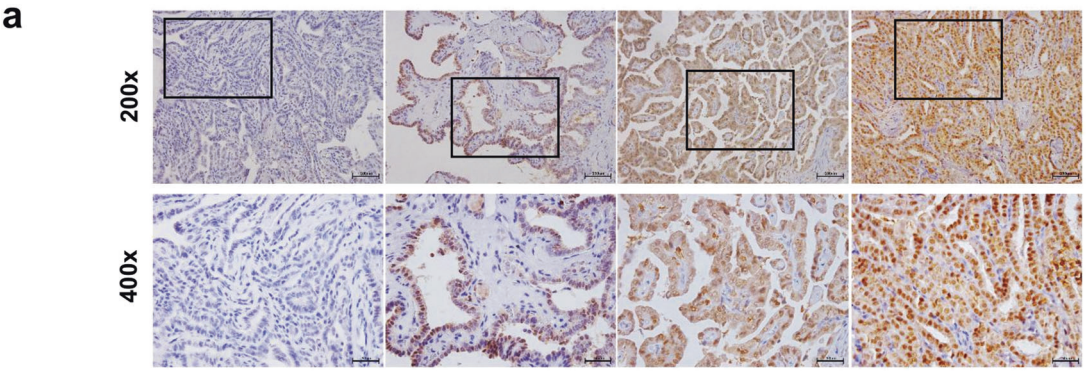

TBX3 expression	Negative	+	++	+++	Total
	Low		Moderate	High	
Normal thyroid tissue	49 (69%)	14(19.7%)	8	0	71
Total	63(88.7%)		8(11.3%)	0(0%)	
thyroid Tumor	18(18.4%)	13(13.3%)	34	33	98
Total	31(31.6%)		34(34.7%)	33(33.7%)	

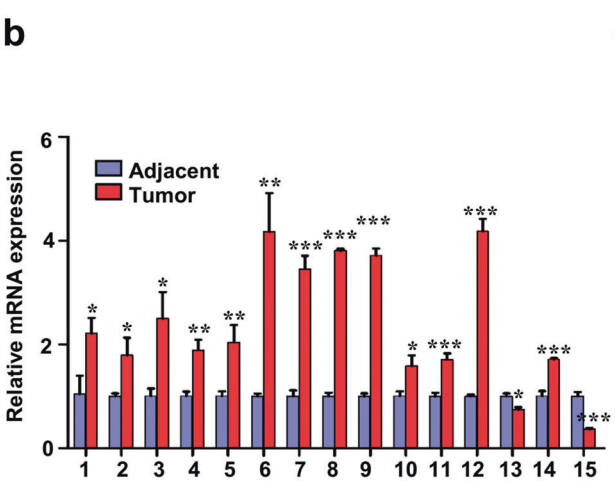

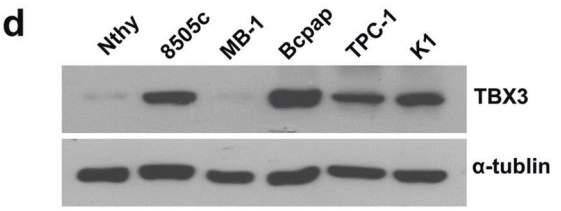

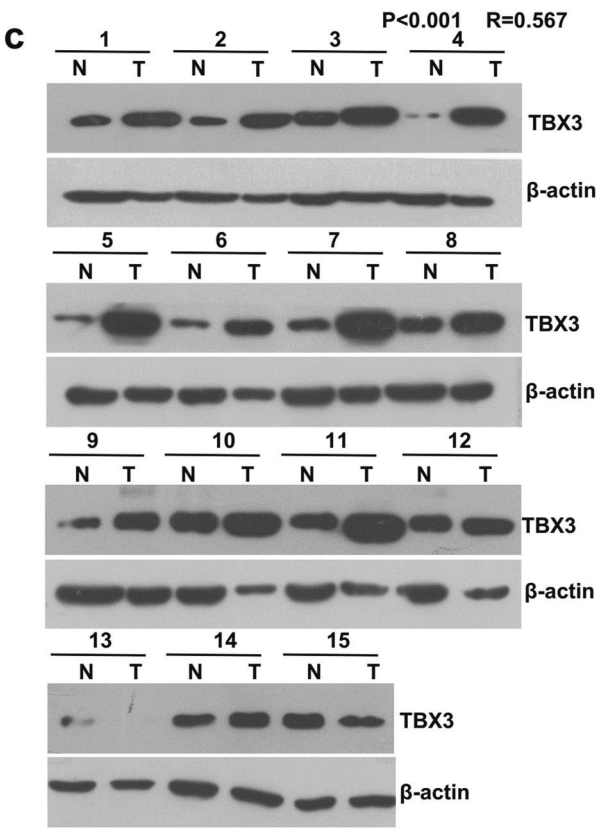

Fig. 1 TBX3 is upregulated in PTC specimens and correlated with cancer progression. **a** Immunohistochemical staining of TBX3 in representative normal thyroid and PTC tissues. Scale bars, 100μm and 50μm, respectively (brown color indicates positive immune reaction). Expression levels of TBX3 were scored as four grades (negative, +, + +, +++) by multiplying the percentage of positive cells and immunostaining intensity. The positively stained nuclei (%) were analyzed by χ^2 test. *R* is the correlation coefficient. **b** Expression of TBX3 at mRNA level in PTC samples was analyzed using qRT-PCR; representative results were shown. Expression of TBX3 in the same PTC samples (**c**) and PTC cell lines (**d**) at protein level was analyzed using western blotting; bars, s.d. $*p < 0.05$, $**p < 0.01$, $***p < 0.001$

cells through repressing tumor suppressor PTEN [16]. Apart from its role in the cell cycle, TBX3 is also known to repress E-cadherin expression in melanoma and colorectal cancer, leading to enhanced invasiveness [8, 17, 18]. TBX3 interacts with several critical pathways associated with cell survival. In liver tumorigenesis, for example, the Wnt–β-catenin pathway induced TBX3 expression which, in turn, mediates β-catenin function [19]. TBX3 functions downstream of estrogen/FGF signaling and expands cancer stem-like cells population in breast cancer [20]. Considering the plentiful biological processes TBX3 contributes to, it must be regulating a number of target genes and interacting with great amount of partner molecules.

Thyroid cancer (TC) is the most common endocrine-related cancer with continuously increasing incidences during the past few decades. Unfortunately, the incidence in children increases most strikingly due to the rapid growth of thyroid in childhood. Papillary thyroid carcinoma (PTC), derived from thyroid follicular cells, is the most common histology subtype and accounts for 80% of all TC cases [21]. PTC is well-differentiated and usually associated with good prognosis and therapeutic response; nevertheless, about 10% of patients die from recurrences and distant metastasis after several years of diagnosis [22]. Although mutations of the MAPK pathway and PI3K–AKT pathway factors, especially BRAF V600E mutation, RET/PTC rearrangement, have been reported in PTC cases, the genetic events underlying the initiation and progression of PTC remain largely unknown [21] Therefore, identification of new molecular targets which will help in early diagnosis and for targeted therapy to manage the growth and survival of malignant cells is necessary.

The biological role and related mechanisms of TBX3 in PTC tumorigenesis have not been studied. In the current study, we found TBX3 promotes the proliferation of PTC cells as well as the tumor formation in vivo through repressing the critical CDK inhibitor p57^{KIP2}. Consistently, expression of TBX3 is upregulated in PTC tumor specimens while negatively correlated with that of p57^{KIP2}. The following mechanism investigation showed that recruitment of PRC2 complex and HDAC1/2 is necessary for the transcriptional repression function of TBX3. These studies advance our understanding of TBX3 function in PTC development and related molecular mechanisms.

Results

TBX3 is upregulated in PTC and correlated with PTC progression and poor prognosis

To evaluate the correlation between TBX3 expression level and thyroid tumor development, we determined the expression of TBX3 in PTC specimens. We collected 98 PTC samples, 71 of them with adjacent normal tissues and performed tissue arrays by immunohistochemical staining. Strikingly, TBX3 was found to be significantly upregulated in tumors compared to the adjacent normal tissue (Fig. 1a). In 13 of 15 selected paired samples of different grade cancers, the mRNA level of TBX3 was also revealed to be higher in tumor than the adjacent tissue, as measured by quantitative real-time RT-PCR (qRT-PCR) (Fig. 1b). Consistently, western blotting further confirmed elevated expression of TBX3 in PTC samples as well as in PTC cell lines (Figs. 1c, d).

The correlations between TBX3 expression and clinicopathologic features are shown in Table 1. The high expression of TBX3 in PTC was significantly correlated with lymph node metastasis ($p < 0.001$) and tumor node metastasis (TNM) stage ($p = 0.022$), but not associated with other factors including age, sex, and tumor size (Table 1).

Table 1 Correlation of TBX3 expression in human PTC with clinicopathologic features

Vairables	$n = 98$	TBX3 expression			*P*-value
		Negative/low	Moderate	High	
Age					0.531
<45		19	21	19	
≥45		12	13	14	
Gender					0.314
Male		4	7	6	
Female		27	27	27	
Tumor size					0.531
≤1 cm		12	15	12	
>1 cm		19	19	21	
LNM					<0.001
No		22	14	6	
Yes		9	20	27	
Multifocality					0.228
No		23	23	20	
Yes		8	11	13	
TNM stage					0.011
I–II		27	25	17	
III–IV		4	9	16	
MEE					0.022
No		27	26	18	
Yes		4	8	15	
T stage					0.007
T1+T2		29	28	19	
T3+T4		2	6	14	

LNM lymph node metastasis, *MEE* minimal extrathyroidal extension, *p*-values were calculated by Pearson's chi-square tests. A value of $p < 0.05$ was considered statistically significant

TBX3 promotes the cell proliferation of PTC cells

To investigate its potential function in PTC tumorigenesis, we first knocked down TBX3 expression using RNA interference in two selected PTC cell lines, K1 and TPC-1. The targeted siRNAs were able to effectively repress TBX3 at mRNA (Supplementary Figure 1a) and protein levels. Both of the PTC cell lines with decreased TBX3 expression had slower growth rates as evaluated by CCK8 assay (Fig. 2a). Then we generated K1 and TPC-1 cells with stable depletion of TBX3 using lentivirus mediated shRNA (shTBX3)(Supplementary Figure 1b). Compared to scrambled shRNA-transduced control cells, the shTBX3 clones grew apparently more slowly (Fig. 2b). Colony formation assays further showed that TBX3 knockdown reduced the number of colonies formed (Fig. 2c). Next, flow cytometry (FACS) experiments were carried out to determine whether the decrease in cell proliferation upon TBX3 knockdown was due to inhibition of cell-cycle progression or cell death. Knockdown of TBX3 resulted in an increase of G1-phase population, and a concomitant decrease of cell number at the S phase and G2/M phase compared with control cells (Fig. 2d). No apparent difference was noticed in the sub-G1 phase cells, suggesting that TBX3 knockdown barely affect apoptosis (data not shown). Consistently, stable knockdown of TBX3 resulted in a similar ratio of G1/S transition arrest (Fig. 2e).

CRISPR/Cas9 system was also employed to knock out *tbx3* gene; cell proliferation examined by both CCK8 and colony formation assays showed comparable results to shRNA clones in K1 and TPC-1 cells (Supplementary Figures 2 and 4a). TBX3 knock out caused G1-phase arrest similarly as the shRNA clones.

In contrast, PTC cells stably overexpressing TBX3 showed increased cell proliferation both in CCK8 and colony formation assays. Overexpression of TBX3 also increased the proportion of S phase and G2/M phase cells (Supplementary Figure 3). Taken together, these experiments suggested that TBX3 promotes PTC cell proliferation and cell-cycle progression.

Identification of $p57^{KIP2}$ as a downstream target of TBX3

TBX3 has been found to promote cell proliferation through repressing cyclin-dependent kinase inhibitor (CKI) $p21^{WAF1/CIP1}$ as well as the activator of p53, $p14^{ARF}/p19^{ARF}$, so as to bypass senescence in breast cancer and melanoma cells. To verify if the similar functional mechanism was adopted in PTC and search for putative TBX3 target genes involved in cell-cycle regulation, we investigated the transcriptomes in TBX3-depleted K1 cells by high-throughput RNA sequencing (RNA-seq). Briefly, total RNA was extracted from K1 cells with stable knockdown of TBX3 and subjected to BGISEQ-500 analysis. With a stringent cutoff (false discovery rate <0.05), RNA-seq identified 802 genes whose expressions were altered upon TBX3 knockdown. Then we carried out functional classification based on the GO terms (biological process) on the 282 up- and 520 downregulated genes specifically in TBX3-depleted K1 cells (Fig. 3a). Genes are involved in multiple biological signaling pathways, especially those critical for cell and organ growth. The detailed results of RNA-seq are provided in Supplementary Table 1 .

We next validated expression of the representative genes implicated in cell proliferation regulation by qRT-PCR in K1 cells. The results indicated that the mRNA levels of MYB, CCNG2, and CKS2 were decreased upon knockdown of TBX3, albeit to distinct extents (Fig. 3b). Similar to functional mechanisms reported under other cancer background, TBX3 knockdown in PTC cells resulted in de-repression of *CDKN1A* gene, which codes for the CDK inhibitor $p21^{WAF1/CIP1}$. Interestingly, the mRNA level of *CDKN1C*, the coding gene for another pivotal CDK inhibitor $p57^{KIP2}$, was also significantly elevated in TBX3-depleted cells (Fig. 3b). At the protein level, expression of $p57^{KIP2}$ showed corresponding increase or decrease in TBX3 knocked down or overexpressed cells respectively (Fig. 3c and Supplementary Figure 4a). To further check if the repression of $p57^{KIP2}$ by TBX3 is a general phenomenon in PTC cells, its expression in TBX3-modulated TPC-1 cells was evaluated and the similar regulation relationship was observed (Supplementary Figure 4a). These results strongly suggest that $p57^{KIP2}$ could be an important downstream function mediator of TBX3 in the PTC tumorigenesis.

To test whether $p57^{KIP2}$ de-repression could be the cause of proliferation retardation in TBX3-depleted cells, we transfected siRNA against *CDKN1C* into K1 cells with stable knockdown of TBX3 and determine whether the G1-phase accumulation could be rescued. FACS analysis revealed that $p57^{KIP2}$ knockdown in TBX3-depleted cells resulted in a significant decrease in the percentage of cells at the G1 phase (Fig. 3d). Similar rescue effect on cell cycle by $p57^{KIP2}$ knockdown was also observed in TBX3 knock out cells (Supplementary Figure 4b). Therefore, $p57^{KIP2}$, by controlling the transition between G1 and S phase, mediates the pro-proliferation function of TBX3 in PTC cells.

TBX3 transcriptionally regulates $p57^{KIP2}$ expression

$p57^{KIP2}$, belonging to Cip/Kip CKIs family, is a critical cell-cycle regulator during embryonic development and also involved in tumorigenesis, but we have not seen any report about its functional correlation with T-box transcription

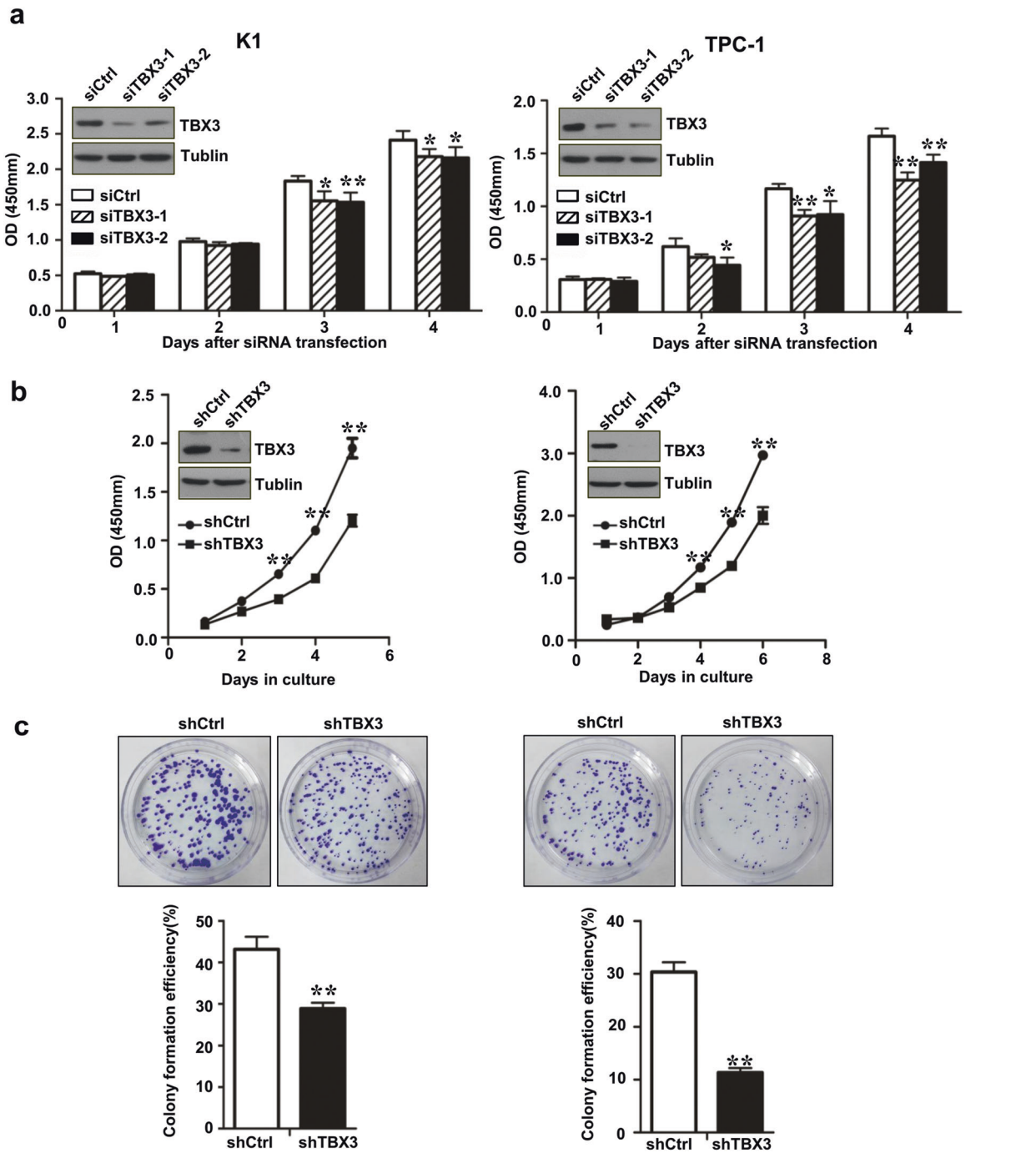

Fig. 2 Suppression of TBX3 induces G1/S transition arrest. **a** K1 (left) and TPC-1 (right) were transiently transfected with siRNA against TBX3 (siTBX3) or control (siCtrl) and then subjected to cell growth assays over a period of 4 days. Columns, mean ($n = 6$); bars, s.d. $^{**}p < 0.01$. **b** K1 (left) and TPC-1 (right) were stably transduced with shCtrl or shTBX3 lentivirus and maintained in culture media with puromycin (3ug/ml) for 14 days before subjected to cell growth assays. Points, mean ($n = 6$); bars, s.d. $^{*}p < 0.05$,$^{**}p < 0.01$. **c** K1 and TPC-1 cells with stable knockdown of TBX3 (shTBX3) or control (shCtrl) were cultured for 14 days prior to crystal violet staining. Representative pictures were shown on the top and the number of colonies was counted. Columns, mean ($n = 3$); bars, s.d. $^{**}p < 0.01$. **d** The fractions of viable cells in the G1, S, and G2–M phases were quantified by flow cytometry. Representative profiles were shown on the left and the percentage of cells was statistically analyzed on the right. **e** Cell-cycle assays were conducted as described above on K1 and TPC-1 cells with stable knockdown of TBX3

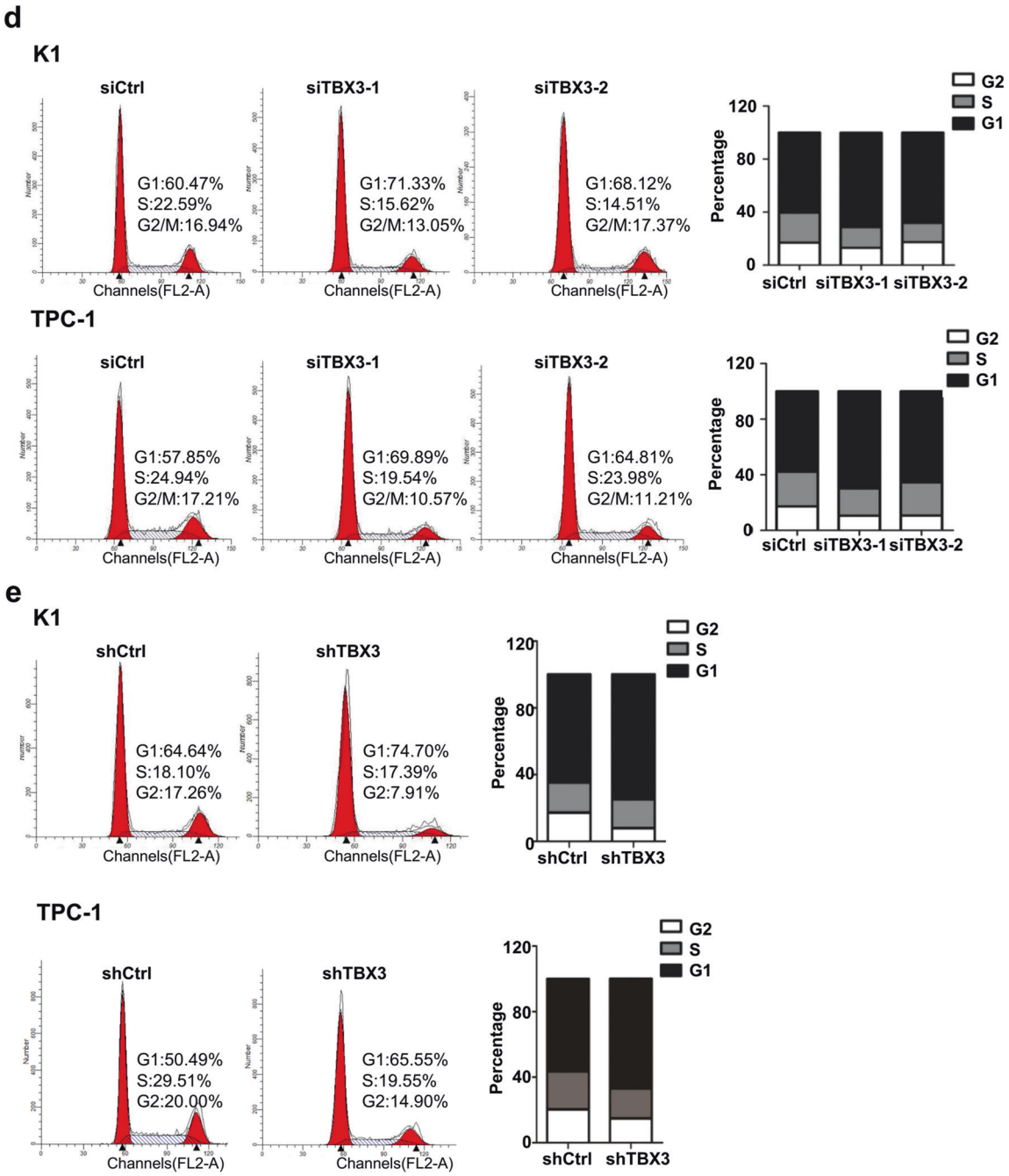

Fig. 2 For legend see previous page

factors. TBX3, like other members of T-box factor family, regulates its downstream targets through direct binding to the "T-half-site" and works as a repressor most of the time. To determine whether TBX3 regulates $p57^{KIP2}$ expression at the transcription level, we cloned the promoter region of *CDKN1C* gene (−2300 to +200bp) upstream the GLUC reporter gene and performed luciferase activity assays. As shown in Fig. 4a, TBX3 repressed the activity of the *CDKN1C* gene promoter in a dose-dependent manner within both HEK293T and K1 cells. To map the cis-element (s) within the *CDKN1C* promoter that is/are required for TBX3-dependent transcription repression, we took advantage of the Jasper database (http://jasper.genereg.net) with the stringency of 80%.

Six potential T-half-site-like elements were assigned to −2262, −1906, −1279, −800, −718, and −363bp position separately. To further validate the importance of these potential sites, HEK293T cells were transfected with a

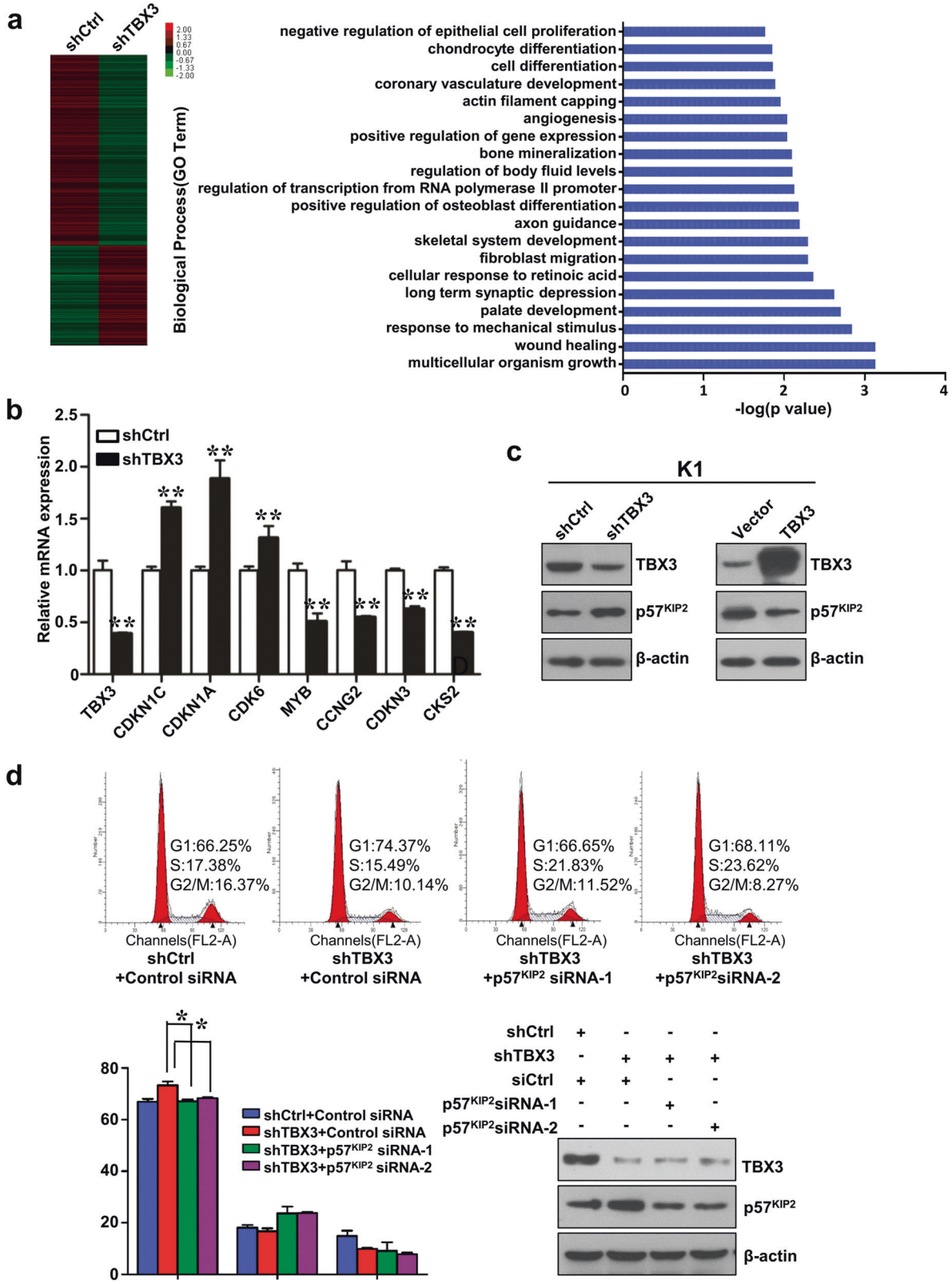

Fig. 3 TBX3 regulates expression of cell-cycle modulator p57^{KIP2}. **a** RNA extraction and deep sequencing were performed on K1 cells with stable knockdown of TBX3 (shTBX3) or control (shCtrl). Regulated genes were grouped and statistically analyzed according to GO pathways. **b** RNA was extracted from K1 cells with stable knockdown of TBX3 and subjected to qRT-PCR of indicated genes. Columns, mean ($n = 3$); bars, s.d. $*p < 0.05$, $**p < 0.01$. **c** Protein expression of p57^{KIP2} was analyzed in K1 cells with stable knockdown or overexpression of TBX3. **d** The effect of p57^{KIP2} knockdown by siRNA transfection on cell proliferation was detected in TBX3 stable knockdown cells

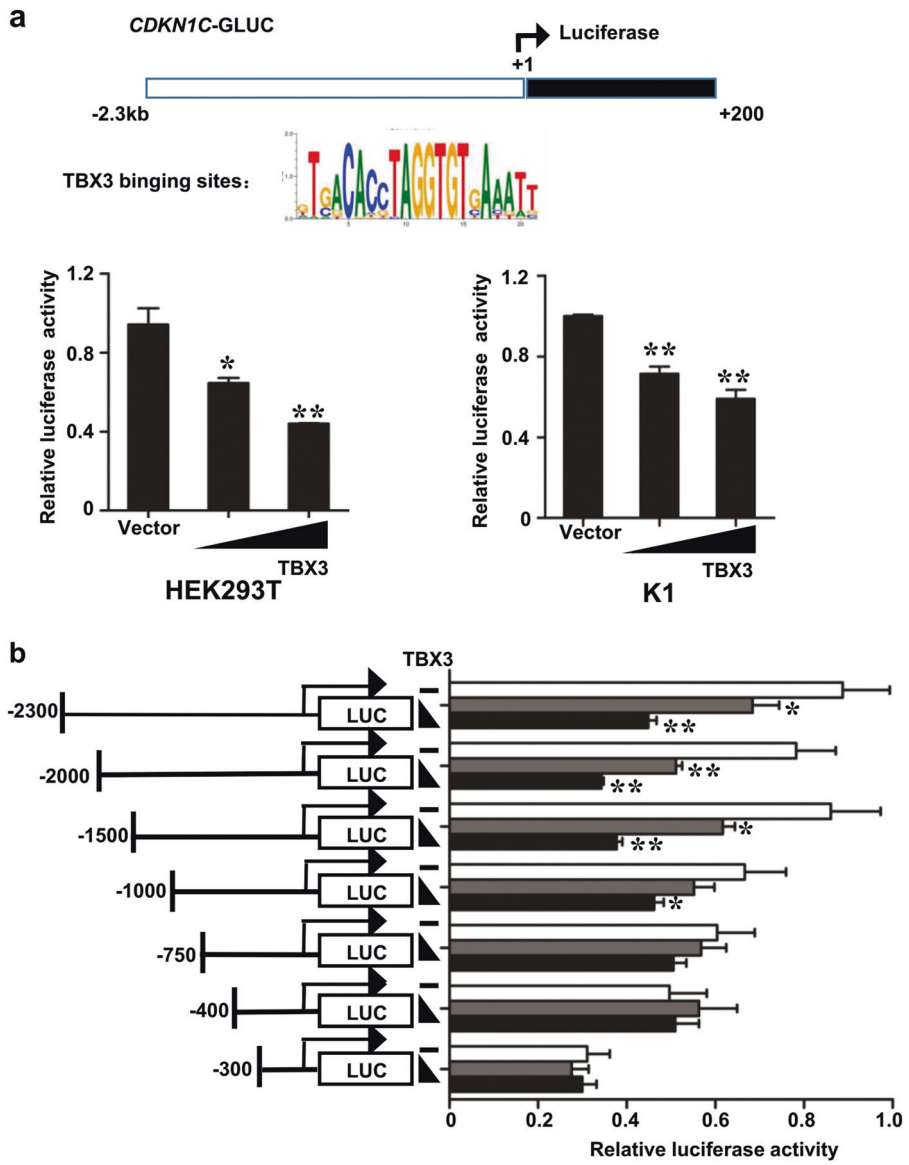

Fig. 4 TBX3 transcriptionally represses $p57^{KIP2}$ expression. **a** K1 (left) and HEK293T cells (right) were co-transfected with *CDKN1C* promoter construct and different amounts of TBX3 expression construct (0.4, 0.8, 1.2 μg) and assayed for GLUC activity using SEAP activity as control. Columns, mean ($n = 3$); bars, s.d. $*p < 0.05$, $**p < 0.01$. **b** Potential TBX3-binding sites within *CDKN1C* promoter were mapped through generating different truncated promoter constructs, co-transfecting with TBX3 and performing GLUC activity assays. Columns, mean ($n = 3$); bars, s.d. $*p < 0.05$, $**p < 0.01$. **c** CHIP experiments were performed using anti-FLAG in K1 cells with stable overexpression of FLAG-tagged TBX3 or anti-TBX3 antibody in normal K1 cells, and followed by qPCR with primers across the regions containing potential TBX3-binding sites in *CDKN1C* promoter. qPCR products were subjected to agarose electrophoresis. **d** DNA affinity binding assays were performed using biotin-labeled probe containing −1279bp or −800bp TBX3-binding sites and K1 nuclear lysate, then followed by western blotting using anti-TBX3 antibody. **e** TBX3-binding sites within *CDKN1C* promoter were mutated and subjected to GLUC activity assay

series of 5′-truncated *CDKN1C* promoter GLUC constructs with the presence of TBX3 and followed by GLUC activity measurements. The repression by TBX3 on the promoter activity became weaker when the truncation went down to −1000 to +200bp, and hardly detectable when it went down to −750 to +200bp, suggesting the predicted binding sites located at −1279 and −800bp could be the actually functional TBX3-binding sites (Fig. 4b). To further verify whether TBX3 represses *CDKN1C* promoter through direct binding, we performed chromatin immunoprecipitation (ChIP) assays. As expected, TBX3 was recruited to both −1279 and −800bp sites, but not to other predicted sites detected by ChIPs with anti-FLAG against K1 cells stably overexpressing FLAG-tagged TBX3 as well as with antibody against endogenous TBX3 (Fig. 4c)

To further assess the association between TBX3 and the above found binding sites within *CDKN1C* promoter, we conducted in vitro DNA affinity binding assay. We

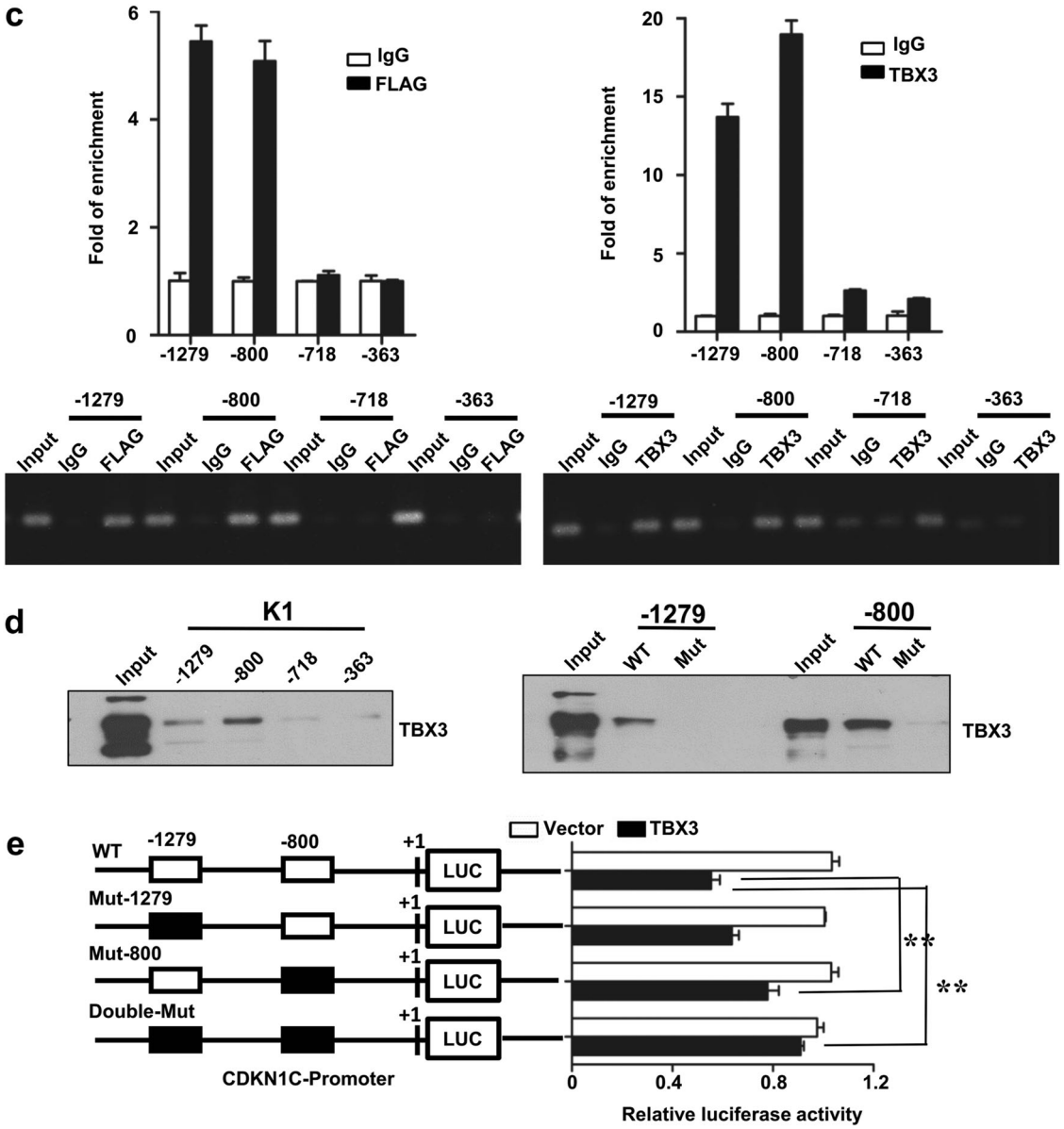

Fig. 4 For legend see previous page

incubated the biotin-labeled DNA probe spanning around −1279bp site or −800bp site with K1 cell lysates, and then TBX3 was efficiently pulled-down as detected by western blotting (Fig. 4d). On the contrary, when mutated probes were employed, direct interaction with TBX3 was no longer detectable within the system. Then we introduced mutation of the two binding sites into GLUC construct respectively or simultaneously to check the effect on promoter activity. Mutation of either site, especially −800bp site, relieved TBX3-mediated transcriptional repression proportionally, while mutation of both sites abrogated the repression dramatically (Fig. 4e). The −800bp site seems to be playing more critical role in terms of direct binding with TBX3 as well as mediating the promoter activity repression (Fig. 4d, e).Taken together, these results demonstrated that TBX3 physically associates with the *CDKN1C* promoter and represses its transcription.

TBX3 is physically associated with PRC2 complex and HDAC1/2

CDKN1C expression is often downregulated in human cancer via promoter DNA methylation; it is recently found that EZH2-mediated histone H3 lysine 27 trimethylation

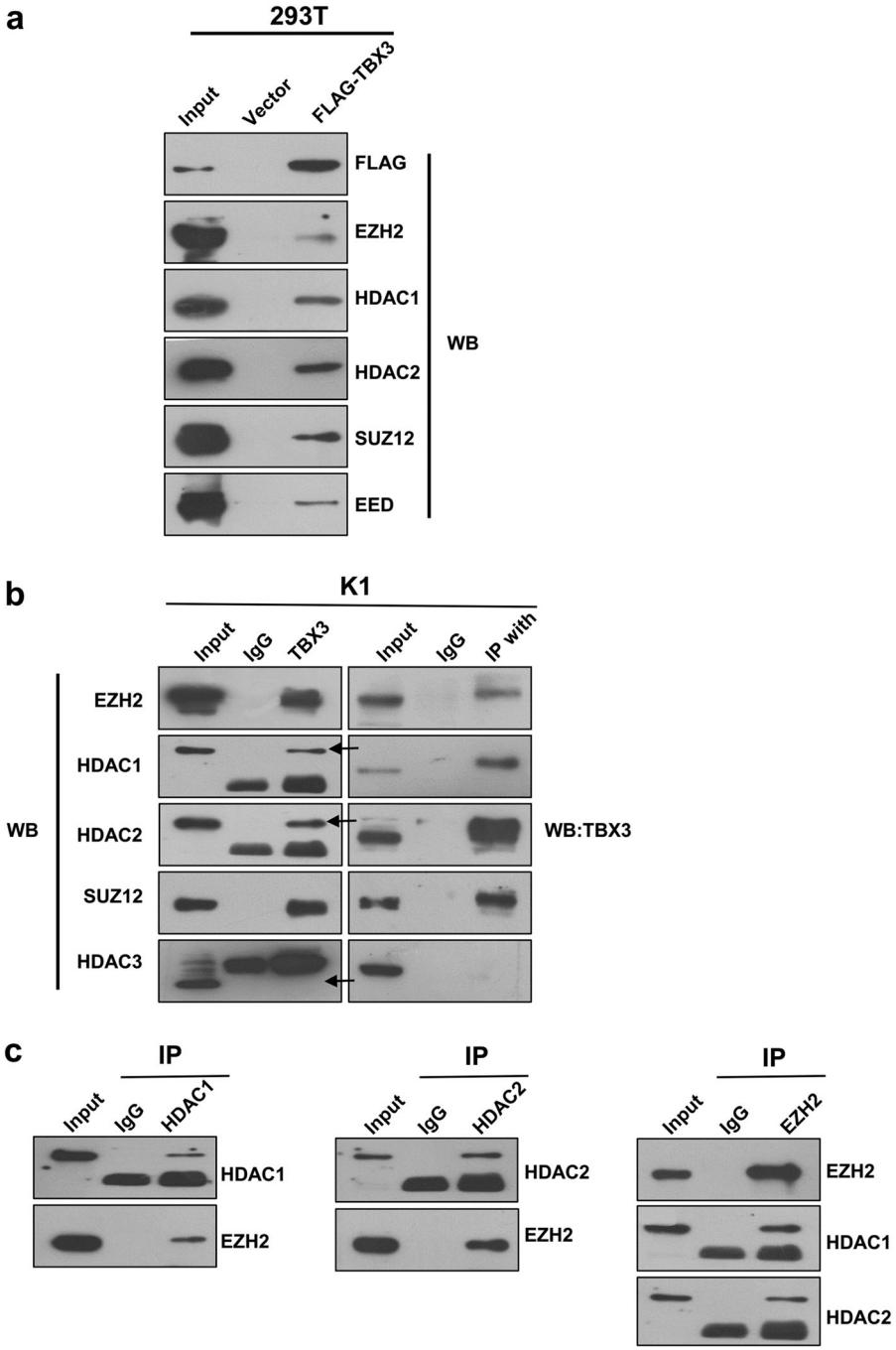

Fig. 5 TBX3 physically associates with PRC2 complex and HDAC1/2. **a** Cell extracts from HEK293T cells expressing FLAG-tagged TBX3 were immunoprecipitated with anti-FLAG and immunoblotted with antibodies against indicated factors. **b** Cell extracts from K1 cells were immunoprecipitated with anti-TBX3 and immunoblotted with indicated antibodies (left panel) or immunoprecipitated with indicated antibodies and immunoblotted with anti-TBX3 (right panel). **c** Cell extracts from K1 cells were immunoprecipitated and immunoblotted with indicated antibodies

(H3K27me3) as well as histone deacetylation was also involved in its repression in breast cancer [23, 24], so we wonder whether related histone modifications are required for TBX3-mediated transcriptional repression. To detect if there is physical interaction between TBX3 and EZH2, as well as other important components of PRC2 complex, EED and SUZ12, cell extracts were obtained from HEK293T cells expressing FLAG-tagged TBX3. Immunoprecipitation (IP) with ani-FLAG followed by immunoblotting (IB) with antibodies against the above factors showed that they were efficiently co-immunoprecipitated with TBX3 (Fig. 5a). Similarly, HDAC1 and HDAC2 were also found to co-immunoprecipitate with TBX3.

To further validate the in vivo interaction between TBX3 and these factors, co-immunoprecipitation experiments were performed on endogenous proteins from K1 cell. IPs were firstly exerted with antibody against TBX3, and followed by IB with antibodies against EZH2/EED/SUZ12, HDAC1&2 respectively. The results indicated that TBX3 was co-immunoprecipitated with EZH2/EED/SUZ12 as

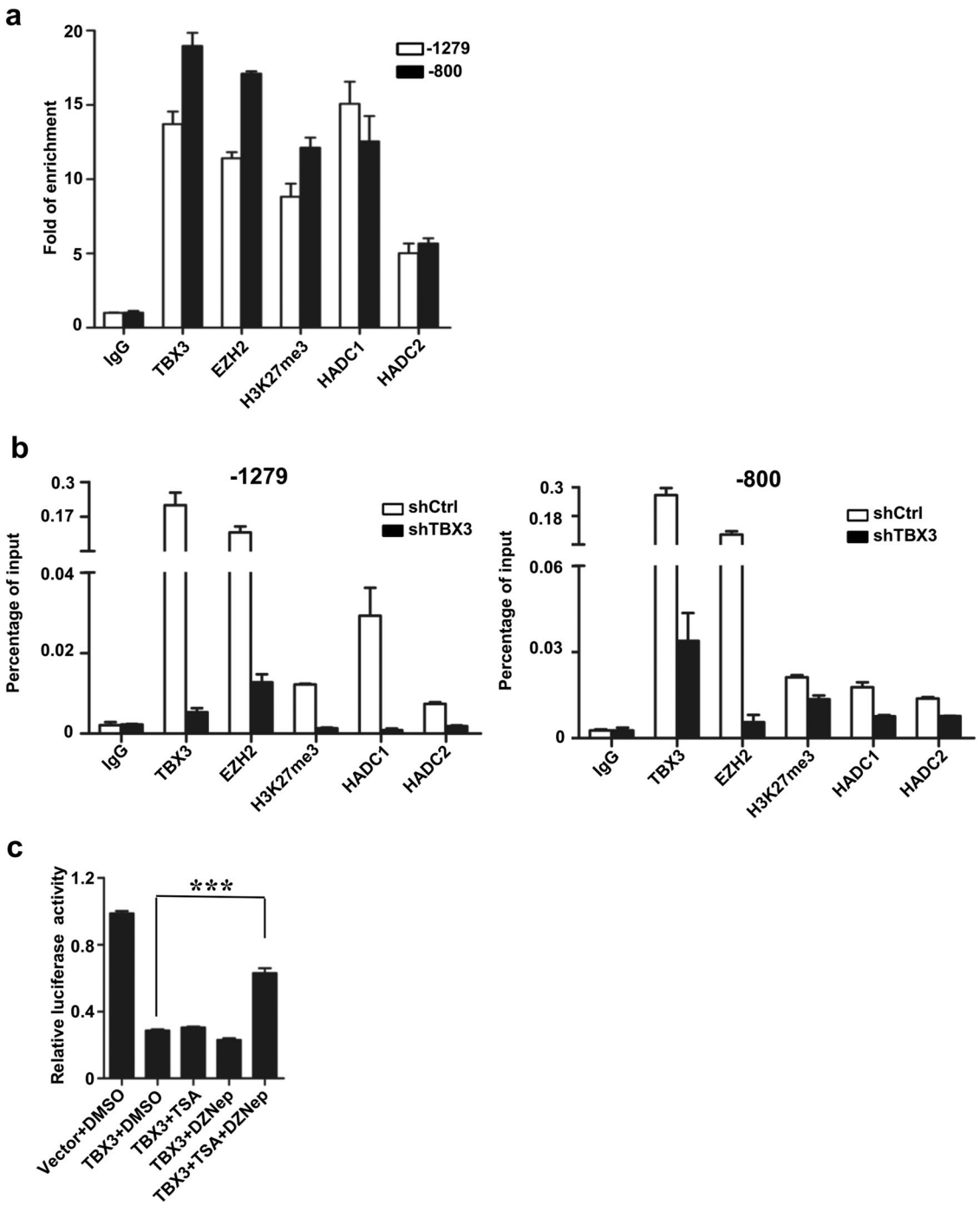

Fig. 6 Recruitment of PRC2 and HDAC1/2 is necessary for transcriptional repression function of TBX3. **a** CHIP experiment was performed using antibodies against indicated factors and followed by qPCR using primers across the region containing TBX3-binding sites in *CDKN1C* promoter. **b** CHIP experiments for indicated factors were performed on K1 cells with stable knockdown of TBX3. **c** HEK293T cells were co-transfected with *CDKN1C* promoter and TBX3 expression constructs with the presence of indicated inhibitors and assayed for relative luciferase activity. Columns, mean ($n = 3$); bars, s.d. $*p < 0.05$, $**p < 0.01$. **d** K1 cells were transfected with TBX3 expression constructs, and incubated with indicated inhibitors followed by western blotting against p57^{KIP2} as well as flow cytometry assays

well as HDAC1/2, but not HDAC3 (Fig. 5b, left panel). Reciprocally, IP with antibodies against EZH2/EED/SUZ12, HDAC1/2 followed by IB with antibody against TBX3 also showed that these proteins were associated with TBX3 (Fig. 5b, right panels). Similarly, EZH2 and HDAC1/2 were also detected to be co-present within regulation complex as confirmed by co-immunoprecipitation (Fig. 5c). Taken together, these experiments showed that TBX3 is

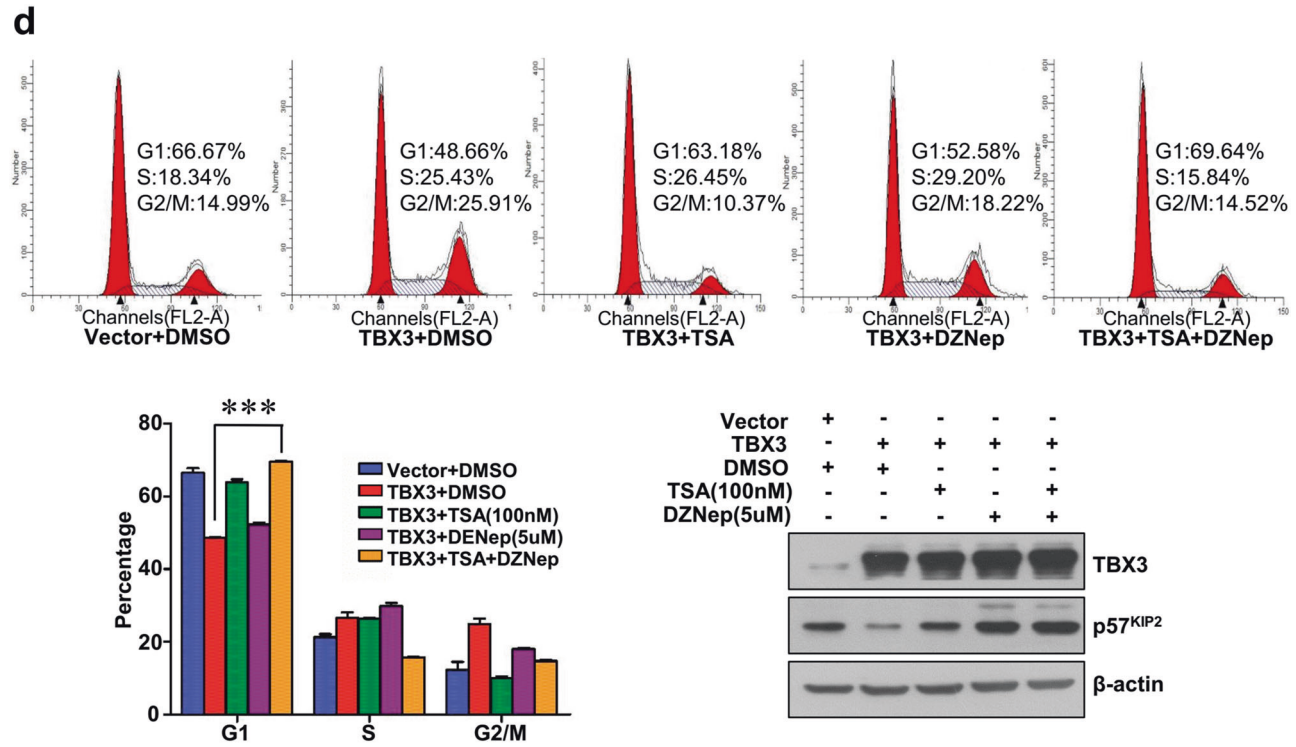

Fig. 6 For legend see previous page

physically associated with PRC2 complex and HDAC1/2 in vivo.

Recruitment of PRC2 and HDAC1/2 is required for TBX3 transcriptionally repression function

As we have found that TBX3 transcriptionally repressed $p57^{KIP2}$ expression and it associated with PRC2 complex as well as HDAC1/2, we wonder if the complex formation is involved in its regulatory function.

Firstly, we checked if PRC2 complex and HDAC1/2 were recruited to *CDKN1C* promoter region by CHIP experiments. As shown in Fig. 6a, EZH2, EED1, and HDAC1/2 occupied the *CDKN1C* promoter, concentrated around −1279 and −800bp regions, corresponding to the TBX3-binding sites identified above. Consequently, H3K27me3 was also found to bind the same regions. However, the recruitment of the PRC2 complex and HDAC1/2 was barely detectable when CHIPs were performed within TBX3-depleted cells, which suggested that the binding of TBX3 on the *CDKN1C* promoter is the prerequisite for histone modification enzymes to aggregate (Fig. 6b).

Functionally, although TBX3 still showed partial repression of *CDKN1C* promoter activity when only DZNep, the specific inhibitor for H3K27me3, or TSA, the specific inhibitor for HDAC1/2, was included in the GLUC activity assays, the repression was dramatically relieved once the two inhibitors were present simultaneously (Fig. 6c). We next found the decreased endogenous $p57^{KIP2}$ protein expression caused by overexpressed TBX3 was also effectively recovered by dual-inhibitor treatments (Fig. 6d). Consistently, although either DZNep or TSA treatment inhibited the proliferation elevation observed in TBX3-overexpressing K1 cells partially, dual-treatment restored it to a level comparable with the control cells (Fig. 6d). Collectively, these data suggest that recruitment of histone modification complex including PRC2 and HDAC1/2 is necessary for the transcriptional repression and pro-proliferation function of TBX3, at least that through $p57^{KIP2}$.

Mutually negative co-relationship between TBX3 and $p57^{KIP2}$

Furthermore, we investigated the importance of TBX3 in PTC development and progression in vivo by implanting TBX3 knockdown or control K1 cells into the subcutaneous sites of nude mice, on the right or left side, respectively ($n = 7$ for each group). Growth of the implanted tumors was monitored by measuring the tumor sizes every 3 days over a period of 3 weeks. The results showed that knockdown of TBX3 level resulted in a dramatic reduction of tumor volume and weight (Fig. 7a–c). Immunohistochemical

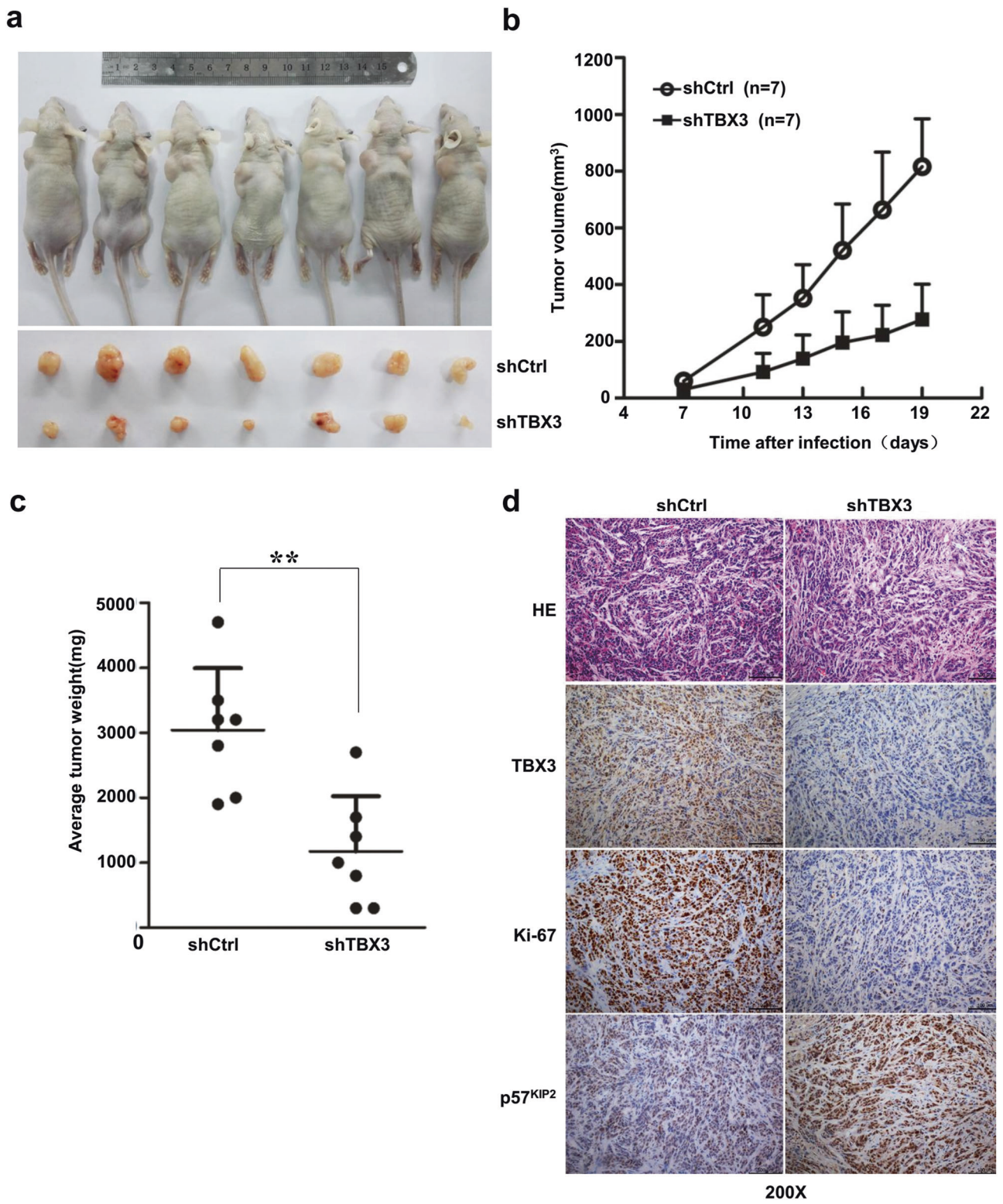

Fig. 7 TBX3-repressed p57^{KIP2} expression is involved in PTC tumorigenesis. **a–c** K1 cells with stable knockdown of TBX3 (shTBX3) or control (shCtrl) were transplanted into athymic mice subcutaneously and tumor sizes were measured every 3 days. Tumor-bearing mice and tumors are shown. The growth curves of tumors were generated and statistically compared. Points, mean ($n = 7$); bars, s.d. $^{**}p < 0.01$. **d** Hematoxylin–eosin and immunohistochemistry stainings of indicated factors were performed on tumor sections harvested from transplantation experiments. **e** Expression of p57^{KIP2} in high grade of PTC samples were analyzed using qRT-PCR, which correspond with samples shown in Fig. 1b (left panel). Additional samples were included, and relative level of TBX3 mRNA expression was plotted against the relative level of p57^{KIP2} expression in 30 pairs of PTC samples(right panel). **f** In all, 482 PTC samples were downloaded from TCGA database to find the correlation of TBX3 and p57^{KIP2}expression

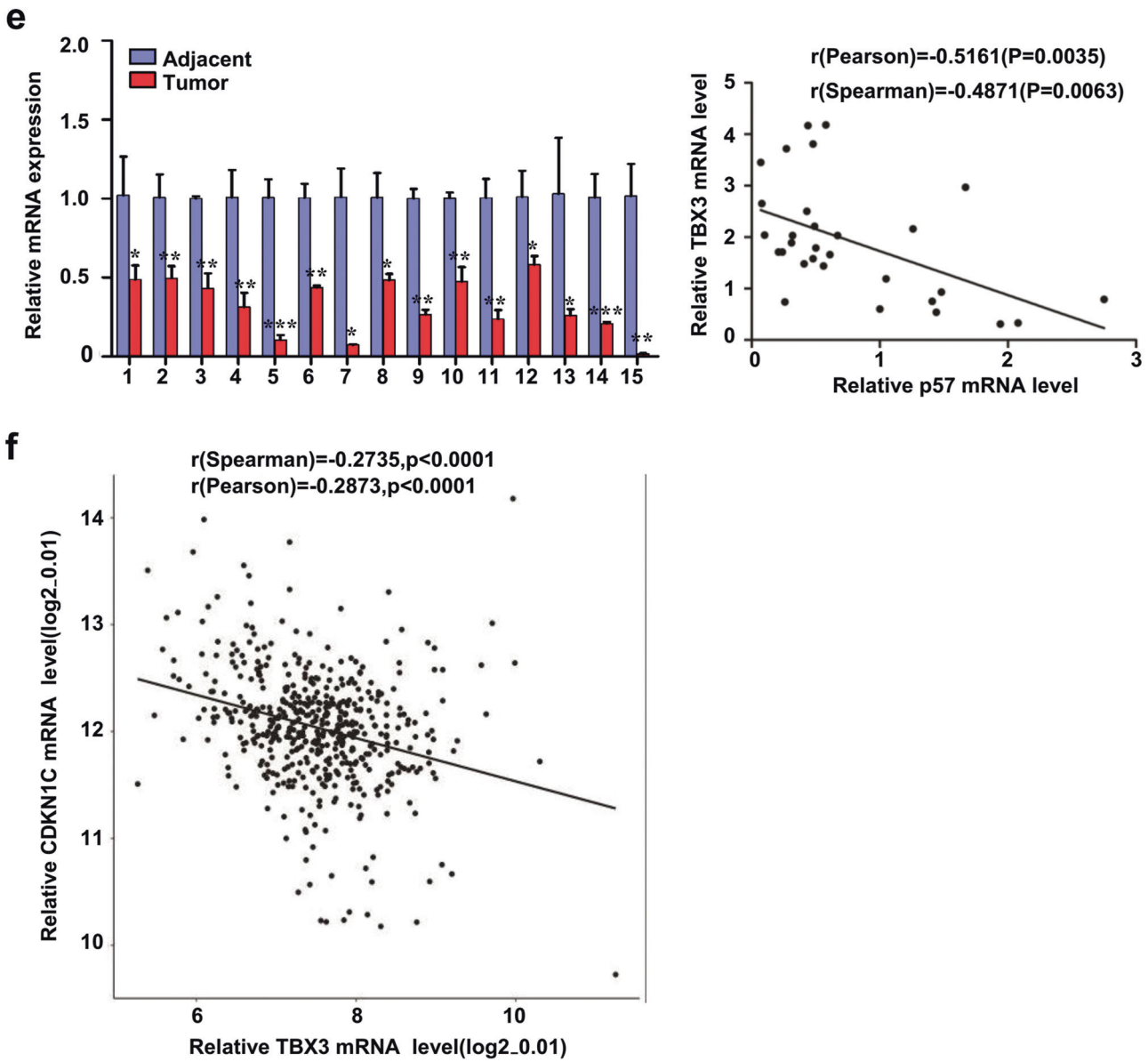

Fig. 7 For legend see previous page

staining first confirmed that TBX3 expression had been maintained at a significantly lower level in TBX3 knockdown tumors (Fig. 7d). Compared with control group, TBX3 knockdown group had fewer Ki67-positive cells, meaning fewer proliferating cells. Remarkably, the expression level of $p57^{KIP2}$ was much higher in TBX3 knockdown tumor samples, which could account for the reduced cell proliferation (Fig. 7d).

In consistent with the in vivo tumorigenesis experiment, $p57^{KIP2}$ expression in PTC specimens is actually negatively correlated with that of TBX3 expression as evaluated by qRT-PCR on the same samples as Fig. 1b. With the increase of sample quantity, we performed statistical analysis and found a Spearman correlation coefficient of -0.4871 ($p < 0.01$) and a Pearson correlation of -0.5161 ($p < 0.01$) when the mRNA level of TBX3 was plotted against that of $p57^{KIP2}$ in 30 paired samples, further confirming the significant negative correlation (Fig. 7e). We next conducted analysis using TCGA dataset, which was shown in Supplementary Table 3, and also found consistent correlationship. We observed that tumors expressing high levels of TBX3 showed statistically significant or tendency toward significant co-occurrence with tumors expressing low level of $p57^{KIP2}$ (Fig. 7f). Taken together, these experiments indicate that TBX3 plays an important role in promoting tumorigenesis and $p57^{KIP2}$ works as a critical downstream target of TBX3 to mediate its pro-proliferation function in PTC development.

Discussion

TBX3 functions as a transcriptional repressor most of the time and has been found to participate in critical biological processes in a broad variety of tumorigenesis. In the current study, we investigated the relationship between TBX3 and PTC development. Immunohistochemistry staining, western blotting, and qRT-PCR analysis demonstrated that high expression of TBX3 was frequently detected in PTC specimens and positively correlated with advanced tumor grade, thus underscoring its potential role as an underlying biological mechanism in the development and progression of PTC.

In melanoma and breast cancer development, TBX3 has been reported to promote tumor cell proliferation through transcriptionally repressing critical tumor-suppressors, including $p14^{ARF}$/$p19^{ARF}$ and $p21^{WAF1/CIP1}$. Phenotypically, we found TBX3 knockdown in PTC cells resulted in G1-phase accumulation therefore decreased proliferation activity in vitro and in vivo. While in the search for downstream targets by RNA-seq analysis, $p57^{KIP2}$, surprisingly, drew our attention. Expression of $p57^{KIP2}$ at both mRNA and protein levels was increased in TBX3 knockdown PTC cells. Although we observed $p21^{WAF1/CAP1}$ expression was elevated by TBX3 depletion as well, knockdown of $p57^{KIP2}$ itself in the same cells was significant enough to relieve the repressed cell proliferation. Apart from this, we were unable to detect expression change of other CKI members. These data suggest that TBX3 promotes proliferation mainly through repressing $p57^{KIP2}$ in PTC cells. It is thus possible that TBX3 fulfills its pro-proliferation function by regulating different CKI family members and related factors under different cancer backgrounds.

As a member of Cip/Kip CKI family, $p57^{KIP2}$ shares a conserved N-termianl domain with the other two members, $p21^{CIP1}$ and $p27^{KIP1}$, but diverges in the remaining sequence, therefore shows distinct function and regulation. It is the only CKI required for embryonic development, as most mice lacking the *cdkn1c* gene have multiple developmental abnormalities and die at birth [25, 26] Recent studies indicate that $p57^{KIP2}$ is frequently repressed in multiple types of human cancers [22, 23] The expression of $p57^{KIP2}$ in thyroid malignancies was investigated by a few groups, but the results are not necessarily homogeneous since different kinds of tumor samples were included [27–29]. In the current study, TBX3 highly expressed PTC samples show decreased expression of $p57^{KIP2}$, which is highly consistent with our molecular functional study. $p57^{KIP2}$ is inactivated in tumors through different mechanisms, including maternal-specific loss of heterozygosity, loss of imprinting, and promoter methylation [30–34]. Based on what we found in this study, direct transcriptional repression of promoter activity could be another mechanism to keep low $p57^{KIP2}$ expression in PTC tumorigenesis. Similarly, transcriptional repression by EWS-FLI-1 was found to be the underlying mechanism to keep Ewing tumor cells actively proliferating [35]. However, whether transcriptional repression by TBX3 is the only mechanism to keep $p57^{KIP2}$ low within PTC cells, or other transcription factors or epigenetic regulation mechanisms are also involved need further investigation.

Regarding the precise role of TBX3 in cell cycle, Willmer et al. [10] recently showed that TBX3 level peaks at S phase and depleting TBX3 leads to an S-phase arrest in chondrosacoma cells. On the contrary, knockdown of TBX2, the highly homologous family member of TBX3, in breast cancer and melanoma cells compromises the S-phase arrest caused by cisplatin induction and results in G2/M arrest. Taken together with our data, TBX3 and TBX2 could be playing slightly different role in cell cycle under different carcinoma background.

Interactions with the main enzyme of PRC2 complex, EZH2, as well as HDAC1/2 were confirmed to be required for TBX3 transcriptional regulating function, at least for repressing *cdkn1c* promoter activity. Consistently, *cdkn1c* was previously found to be targeted by EZH2-mediated H3K27me3 in synergy with HDACs [23, 24]. HDAC function is also required for Tbx3 to repress the promoter activity of $p14^{ARF}$ [13]. These findings deciphered the molecular action mechanism of TBX3 employed in its transcription regulation. As a transcriptional repressor, binding to the consensus T-half-site is the pre-requisite, while recruitment of repression complexes such as PRC2, HDACs may be the button to initiate the repression. We indeed found that the abundance of PRC2 complex components and HDAC1/2 at *cdkn1c* promoter greatly decreased after TBX3 knockdown. Clearly, future investigations are needed to explore the scope and the exact molecular mechanisms of the formation of the TBX3/PRC2/HDAC1/2 complex, and to determine whether this functionality involves additional elements.

TBX3, together with TBX1 and TBX2, has been shown to be required for the proper development of pharyngeal, which is the anlage of parathyroid [36]. And thyroid derives from TBX3 expressing foregut [37]; therefore, it would be helpful to investigate TBX3 function during later development stages to correlate with its function in PTC development. As a critical transcription factor, how its expression and function is regulated and what upstream signalings are involved are all open questions.

Although radiation is the most common etiologic factor for PTC, genetic susceptibility is another important contributor. 40% - 70% of PTC cases harbor the *BRAF* V600E mutation rendering the constitutive active formation of BRAF, which has proven to be associated with unfavorable

features including lymph node and distance metastasis [21]. Taken the possible important function of TBX3 in thyroid and parathyroid development and thyroid tumorigenesis, it would be reasonable to explore the related genetic mutations or copy number variations of it in PTC patients even that of $p57^{KIP2}$. Promoter demethylation could also be a cause of TBX3 overexpression in TC, and needs to be systematically studied. Additionally, whether TBX3 or $p57^{KIP2}$ expression level has any correlation with BRAF (V600E) stratification, or involvement of these two novel factors in PTC diagnosis would provide more meaningful information regarding the tumor grades and prognosis would also be worth studying.

Collectively our study demonstrates that TBX3 plays an essential role in PTC progression. TBX3 is able to promote cell proliferation and tumorigenesis of PTC possibly by facilitating the G1/S transition in the cell cycle. We identified $p57^{KIP2}$ as a novel downstream target of TBX3 in PTC and showed that TBX3 represses expression of $p57^{KIP2}$ through recruiting PRC2 and HDAC1/2 chromatin modification complex. These results will further our understanding of the oncogenic potential of TBX3, which will be useful for the diagnosis and therapy of PTC.

Materials and methods

Tissue specimen and immunohistochemistry

Patient tissues of PTC were obtained from Tianjin cancer institute and hospital (Tianjin, China) under protocols approved by the Ethics Committee of Tianjin Medical University. Samples were frozen in liquid nitrogen immediately after surgeries and maintained at −80 °C until analysis. Samples were fixed in 4% paraformaldehyde (Sigma-Aldrich) at 4 °C overnight before embedded in paraffin and sectioned at 8 μm. Immunohistochemistry was performed according to standard protocols, Briefly, sections were incubated with the polyclonal rabbit anti-human TBX3 antibody (1:400, ABE807; Millipore, Billerica, MD), visualized with DAB Substrate Kit (MaiXin Bio), and monitored with a light microscope. Protein expression levels of all the samples were scored as four grades (negative,+, ++, +++) by multiplying the percentage of positive cells and immunostaining intensity. Basically, the percentage was scored: non-positive cells as 0 point, 1–30% as 1 point, 31–60% as 2 points, 61–80% and 81–100% as 3 and 4 points, respectively. The intensity of staining was scored: no positive staining as 0 point, weak staining as 1 point, moderate staining as 2 points, strong staining as 3 points. The final score were obtained according to above terms: 0 point was no expression, 1–3 was low expression, 4–8 was moderate expression, and 9–12 was high expression.

Cell culture and stable cell line establishment

K1 and TPC-1 PTC cell lines were obtained from Tianjin cancer institute and hospital and respectively maintained in RPMI 1640 or Dulbecco's modified Eagle's medium (DMEM) medium supplemented with 10% fetal bovine serum (Gibco BRL, Gaithersburg, MD). HEK293T were purchased from the American Type Culture Collection (ATCC) and cultured in DMEM medium supplemented with 10% fetal bovine serum (Hyclone, Logan, Utah) and 1% penicillin/streptomycin. All cells were maintained in a humidified incubator equilibrated with 5 % CO_2 at 37 °C.

For the generation of TBX3 stably knockdown cell lines, we produced lentivirus particles by cotransfection of HEK293T cells with recombinant lentiviral vector containing the shTBX3 sequence (5′-CCGGGCTGATGACTGTCGTTATAAACTCGAGTTTATAACGACAGTCATCAGCTTTTTG-3′) or the shCtrl sequence together with packaging plasmids, respectively. For the generation of TBX3 stably overexpression cell lines, lentivirus particles were produced by cotransfection of HEK293T cells with recombinant lentivirals vector containing FLAG-tagged TBX3 cDNA together with packing plasmids. Stably transduced K1 or TPC-1 cells were selected under puromycin. Two small interfering RNAs (siRNAs) against TBX3 (SI03100426; SI00083496) or $p57^{KIP2}$ (SI02654652; SI02654645) were purchased from Qiagen (Qiagen, Hidden, Germany) and transfected into the cells using HiPerFect according to the manufacturer's instructions. Effective knockdown or overexpression of TBX3 was confirmed by western blotting.

CRISPR/Cas9 gene targeting

Guide sgRNAs to target the exon3 of human *tbx3* gene were designed using the Zhang laboratory web resource (http://crispr.mit.edu). The sgRNA encoding oligonucleotides were cloned into lentiGuide-Puro vector (addgene, #52963) using standard procedures, sequence was 5′-GCTCTTACAATGTGGAACCG-3′, and lentivirus particles were produced. K1 and TPC-1 cells were firstly infected with cas9 lentivirus (lentiCas9-Blast, #52962), stable clones were obtained through blastincidin selection. Then K1-cas9 and TPC-1-cas9 cells were infected with lentivirus containing sgRNA and selected with puromycin. Single cell sorting was performed and individual clones were expanded and screened for frameshift mutations. In brief, a region spanning the target site was amplified from genomic DNA of each clone and sequenced. Only the clones with

frameshifting indel mutations while no detectable WT allele were used for subsequent validation and in vitro assays.

Antibodies and western blotting

Whole-cell lysates were prepared with RIPA lysis buffer (Solarbio, Beijing, China) supplemented with proteinase inhibitors cocktail (Roche). Protein concentrations were measured using the Pierce BCA Protein Assay Kit (Pierce, Rockford, lL, USA). Protein lysates were separated by sodium dodecyl sulfate polyacrylamide gel electrophoresis (SDS-PAGE) and target proteins were detected by western blot analysis with antibodies. The sources of antibodies were: anti-TBX3 (ABE807; Millipore, Billerica, MD), anti-TBX3 (42-4800; Invitrogen, Camarillo, CA), anti-Ki-67 (ab16667), anti-P57^{Kip2} (ab75974), Anti-HDAC1 (ab7028), Anti-HDAC2 (ab7029), Anti-HDAC3 (ab32369) (Abcam, Cambridge, MA); anti-EZH2 (#5246), anti-H3K27Me3 (#9733), anti-SUZ12 (#3737) (CST, Danvers, MA), anti-EED (61203, active motif, Carlsbad, CA), anti-Flag (F3165), anti-tublin(T5168), anti-actin (A5441) (Sigma-Aldrich, St. Louis, MO).

Plasmids and reporter activity assay

The 2.5 kb full-length or truncated human *CDKN1C* promoter was inserted into the GLUC reporter plasmid which contains the Gaussia Luciferase (GLUC) and Secreted Alkaline Phosphatase (SEAP) reporter gene (Gene Copoeia., Guangzhou China). HEK293T cells were co-transfected with different promoter reporter constructs and TBX3 expression plasmid or corresponding vector control. Cell culture media were collected and subjected to luciferase activity assays 48h post-transfection. Each experiment was performed in triplicate and repeated at least three times. The mutation plasmids were constructed according to the Fast Mutageneis System (Trans Gen, Beijing, China); PCR cycling conditions were 98 °C for 5 min, 18 cycles of 98 °C for 15 s, 62 °C for 15 s, and 72 °C for 7 min. Mutation primers were designed as follows:

−1279-F:
TCCAACAAAGTTCTGACAGTCCCCATCC
−1279-R:
TGTCAGAACTTTGTTGGAGGGTCCAGCA
−800-F: CTCTCAAAAGTTCCCACACATGGTCCCT
−800-R:
TGTGGGAACTTTTGAGAGACTCCCACCA

Cell proliferation assays

Cells were seeded in quadruplicate in 96 wells at approximately 1000 cells per well, and cell proliferation was assessed using the Cell Counting Kit-8 (Dojindo, Shanghai, China) after 7-day of culture. Cell growth curves were constructed by GraphPad Prism 5. Cells were plated in 6 cm dish at the density of 500 cells per well and cultured for 14 days before stained 0.5% crystal violet (A600331; Sangon Biotech, Beijing, China). The colonies with more than 50 cells was manually counted.

Flow cytometry analysis

For cell-cycle analysis, PTC cells were seeded in 6-well plate at approximately 40% confluence. Cells were harvested and fixed with 70% ice-cold ethanol overnight when confluence reaches 80%–90%. DNA was stained with propidium iodide (50 μg/ml) together with RNase treatment (100 μg/ml) before being analyzed by flow cytometer (BD FACSVerse™ System, San Jose, CA).

Real-time quantitative RT-PCR

Total RNA was isolated using TRIzol reagent (10296028; Invitrogen) according to the manufacturer's instructions. Reverse transcription was performed using 2 μg of RNA by transcriptor First Strand cDNA Synthesis Kit (04 896 866 001; Roche). Quantitative real-time PCR was performed using Roche FastStart Universal SYBR Green Master (04 913 850 001; Roche) in a total volume of 20 μl on ABI-Step one Plus (Applied Biosystems, Foster City, CA). The fold change of gene expression was presented by the $2^{-\Delta\Delta Ct}$ method. Experiments were repeated at least twice in triplicate. Primer sequences were listed in supplementary Table 2.

Immunoprecipitation

Total lysates of K1 cells stably infected with lentivirus generated from FLAG-tagged vector (Control) and FLAG-tagged TBX3 (FLAG-TBX3) were collected with Nonidet P40 lysis buffer (50 mM Tris-HCl, pH 7.4, 150 mM NaCl, 0.5% Nonidet P-40, 2 mM EDTA) supplemented with protease inhibitors. Equal amounts of whole-cell lysates were applied to conjugate anti-FLAG affinity agarose gel (A2220; Sigma-Aldrich) respectively overnight at 4 °C in a roller. After binding, the column was washed with cold 0.2% Nonidet P-40 lysis buffer and eluted with Flag peptide (F4799; Sigma). 5% of the total cell lysates was used as input. The eluates were used by SDS-PAGE using different antibodies.

For endogenous IP assays, K1 cells were washed with cold phosphate-buffered saline and lysed with nuclei lysis buffer (20 mM Tris-HCl, pH 8.0, 5% glycerol, 0.2 mM EDTA, 400 mM NaCl,1.5 mM $MgCl_2$) in the presence of protease inhibitors Cocktails on a rotator at 4 °C for 1 h. For single reaction, 30 μl Protein A/G agrose beads were

incubated with the indicated primary antibody (1–5 μg) for 3–4 h at 4°C followed by incubation with 1 mg nuclear extracts overnight. The recovered complexes were washed 4–6 times with PBST before being added in 2× loading buffer. Then the boiled samples were analyzed by SDS-PAGE with appropriate antibodies.

Chromatin immunoprecipitation

ChIPs were performed in cells as descried previously [38]. Briefly, cells were cross-linked by 1% formaldehyde, sonicated, pre-cleared, and incubated with 4–8 μg of specific antibody per reaction. Protein–DNA complexes were bound to Protein A/G Agrose beads, washed with different concentrations of salt buffers, then the pulled-down DNA was extracted, precipitated, and subjected to qPCR with specific primers. The primers were used as follows:

−1279-F: TCACAGGCTCACCTGAGATA
−1279-R: TGGCCCACCTACCATGA
−800-F: TCCGCAGATAGCGGCTTCAG
−800-R: TCAGCTCCACTCTTTCCCCG.
−718-F: GGGAAAGAGTGGAGCTGAC
−718-R: GCTGGTGTCCCTTCGAG
−363-F: CGCCTGCAGACAAAGGA
−363-R: GGGCGGGAGTTAAAGGG

DNA affinity immunoblot assay

Biotinylated DNA probe was incubated with M-280 Streptavidin Dynabeads (11205D; Invitrogen) in binding buffer (20 mM Tris-HCl pH 7.4, 50 mM NaCl, 1 mM EDTA, 10% glycerol, and 10 ng/μl poly(dI-dC), 1 mM spermidine, 1% bovine serum albumin) for 6 h at 4 °C, followed by addition of K1 nuclear extracts on a rotator overnight at 4 °C. After binding, the DNA-bound protein complexes were washed with binding buffer five times and boiled in protein loading buffer (0.25 M Tris-HCl, pH 6.8,10% SDS, 5% β-mercaptoethanol, 0.05% Bromophenol blue and 50% glycerol). Denatured samples were analyzed by SDS-PAGE using Rabbit polyclonal TBX3 antibody (Invitrogen).

Biotinylated DNA oligos were:

−1279-WT:

5′-biotin-atgggctgctggaccctccaacaggtgtctga-cagtccccatcccgatctgggaggctc-3′

−1279-MUT:

5′-biotin-atgggctgctggaccctccaacaaagttctga-cagtccccatcccgatctgggaggctc-3′

−800-WT:

5′-biotin-gggggctggtgggagtctctcaaggtgtcccaca-catggtccctcggggaaagagtgga-3′

−800-MUT:

5′-biotin-gggggctggtgggagtctctcaaaagttcccaca-catggtccctcggggaaagagtgga-3′.

−718-WT:

5′-biotin-actcgagggccttagggccagcaggtgtgtgagggctc-caggcgcgcggagccctcgaa

−363-WT:

5′-biotin-ggcgaggggcggggcgtcgcggtgtcacgttaccgcccg-cagcgccctttaactcccg

RNA sequencing

Transcriptome data sets are available at the NCBI Gene Expression Omnibus with accession number of GSE106306 and the analysis results with cutoff (p-value ≤0.01, false discovery rate <0.05, fold change >1.5) are provided in Supplementary Table 1. Cluster 3.0 and david (https://david.ncifcrf.gov/tools.jsp) was used in the analysis. Two biological replicates for each sample were included in this experiment.

Tumor xenografts

Six–eight-week-old male BALB/c nude mice were purchased from Beijing Vital River Laboratory Animal Technology Company (Vital River, Beijing, China), and were acclimated for 7 days in the animal facility before experiments. 1×10^6 K1 cells stably transfected with shTBX3 or scrambled control shRNA were injected subcutaneously into the dorsal flanks of the mice ($n = 7$). Volumes were measured approximately every 3 days and calculated according to the following formula: Volume (mm^3) = 1/2 × length × width^2. Mice were sacrificed and tumor tissues were collected once tumor length reaches 12.5 mm. Hematoxylin–eosin staining and immunohistochemistry were performed on processed and sectioned tissues. All procedures were approved by the Animal Care Committee of Tianjin Medical University.

Statistical analysis

All data are expressed as the mean ± sd from three independent experiments, unless specified, each performed at least in triplicate. Statistical significance was evaluated with two tailed paired t-test by using SPSS 17.0 software. A p-value of <0.05 was considered significant.

Acknowledgements This research work was supported by the grants from the National Natural Science Foundation of China (31371329 to L.Z., 81702710 to S.Y., 81472580 to M.G.). Innovation Team Development Plan of the Ministry of Education (IRT13085), The Tianjin Municipal Science and Technology Commission (13JCYBJC37200 to L,Z., 17JCQNJC11200 to S.Y.).

Compliance with ethical standards

Conflict of interest The authors declare that they have no competing interests.

References

1. Bamshad M, Lin RC, Law DJ, Watkins WC, Krakowiak PA, Moore ME, et al. Mutations in human TBX3 alter limb, apocrine and genital development in ulnar-mammary syndrome. Nat Genet. 1997;16:311–5.
2. Douglas NC, Papaioannou VE. The T-box transcription factors TBX2 and TBX3 in mammary gland development and breast cancer. J Mammary Gland Biol Neoplasia. 2013;18:143–7.
3. Trowe MO, Zhao L, Weiss AC, Christoffels V, Epstein DJ, Kispert A. Inhibition of Sox2-dependent activation of Shh in the ventral diencephalon by Tbx3 is required for formation of the neurohypophysis. Development. 2013;140:2299–309.
4. Fan W, Huang X, Chen C, Gray J, Huang T. TBX3 and its isoform TBX3+2a are functionally distinctive in inhibition of senescence and are overexpressed in a subset of breast cancer cell lines. Cancer Res. 2004;64:5132–9.
5. Lomnytska M, Dubrovska A, Hellman U, Volodko N, Souchelnytskyi S. Increased expression of cSHMT, Tbx3 and utrophin in plasma of ovarian and breast cancer patients. Int J Cancer. 2006;118:412–21.
6. Lyng H, Brovig RS, Svendsrud DH, Holm R, Kaalhus O, Knutstad K, et al. Gene expressions and copy numbers associated with metastatic phenotypes of uterine cervical cancer. BMC Genom. 2006;7:268.
7. Perkhofer L, Walter K, Costa IG, Carrasco MC, Eiseler T, Hafner S, et al. Tbx3 fosters pancreatic cancer growth by increased angiogenesis and activin/nodal-dependent induction of stemness. Stem Cell Res. 2016;17:367–78.
8. Rodriguez M, Aladowicz E, Lanfrancone L, Goding CR. Tbx3 represses E-cadherin expression and enhances melanoma invasiveness. Cancer Res. 2008;68:7872–81.
9. Wansleben S, Peres J, Hare S, Goding CR, Prince S. T-box transcription factors in cancer biology. Biochim Biophys Acta. 2014;1846:380–91.
10. Willmer T, Peres J, Mowla S, Abrahams A, Prince S. The T-Box factor TBX3 is important in S-phase and is regulated by c-Myc and cyclin A-CDK2. Cell Cycle. 2015;14:3173–83.
11. Li J, Weinberg MS, Zerbini L, Prince S. The oncogenic TBX3 is a downstream target and mediator of the TGF-beta1 signaling pathway. Mol Biol Cell. 2013;24:3569–76.
12. Lingbeek ME, Jacobs JJ, van Lohuizen M. The T-box repressors TBX2 and TBX3 specifically regulate the tumor suppressor gene p14ARF via a variant T-site in the initiator. J Biol Chem. 2002;277:26120–7.
13. Yarosh W, Barrientos T, Esmailpour T, Lin L, Carpenter PM, Osann K, et al. TBX3 is overexpressed in breast cancer and represses p14 ARF by interacting with histone deacetylases. Cancer Res. 2008;68:693–9.
14. Platonova N, Scotti M, Babich P, Bertoli G, Mento E, Meneghini V, et al. TBX3, the gene mutated in ulnar-mammary syndrome, promotes growth of mammary epithelial cells via repression of p19ARF, independently of p53. Cell Tissue Res. 2007;328:301–16.
15. Willmer T, Hare S, Peres J, Prince S. The T-box transcription factor TBX3 drives proliferation by direct repression of thep21 (WAF1) cyclin-dependent kinase inhibitor. Cell Div. 2016;11:6.
16. Burgucu D, Guney K, Sahinturk D, Ozbudak IH, Ozel D, Ozbilim G, et al. Tbx3 represses PTEN and is over-expressed in head and neck squamous cell carcinoma. BMC Cancer. 2012;12:481.
17. Boyd SC, Mijatov B, Pupo GM, Tran SL, Gowrishankar K, Shaw HM, et al. Oncogenic B-RAF(V600E) signaling induces the T-Box3 transcriptional repressor to repress E-cadherin and enhance melanoma cell invasion. J Invest Dermatol. 2013;133:1269–77.
18. Shan ZZ, Yan XB, Yan LL, Tian Y, Meng QC, Qiu WW, et al. Overexpression of Tbx3 is correlated with epithelial-mesenchymal transition phenotype and predicts poor prognosis of colorectal cancer. Am J Cancer Res. 2015;5:344–53.
19. Renard CA, Labalette C, Armengol C, Cougot D, Wei Y, Cairo S, et al. Tbx3 is a downstream target of the Wnt/beta-catenin pathway and a critical mediator of beta-catenin survival functions in liver cancer. Cancer Res. 2007;67:901–10.
20. Fillmore CM, Gupta PB, Rudnick JA, Caballero S, Keller PJ, Lander ES, et al. Estrogen expands breast cancer stem-like cells through paracrine FGF/Tbx3 signaling. Proc Natl Acad Sci USA. 2010;107:21737–42.
21. Lloyd RV, Buehler D, Khanafshar E. Papillary thyroid carcinoma variants. Head Neck Pathol. 2011;5:51–6.
22. Sato N, Matsubayashi H, Abe T, Fukushima N, Goggins M. Epigenetic down-regulation of CDKN1C/p57KIP2 in pancreatic ductal neoplasms identified by gene expression profiling. Clin Cancer Res. 2005;11:4681–8.
23. Yang X, Karuturi RK, Sun F, Aau M, Yu K, Shao R, et al. CDKN1C (p57) is a direct target of EZH2 and suppressed by multiple epigenetic mechanisms in breast cancer cells. PLoS ONE. 2009;4:e5011.
24. Sun CC, Li SJ, Li G, Hua RX, Zhou XH, Li DJ. Long intergenic noncoding RNA 00511 acts as an oncogene in non-small-cell lung cancer by binding to EZH2 and suppressing p57. Mol Ther Nucleic Acids. 2016;5:e385.
25. Yan Y, Frisen J, Lee MH, Massague J, Barbacid M. Ablation of the CDK inhibitor p57Kip2 results in increased apoptosis and delayed differentiation during mouse development. Genes Dev. 1997;11:973–83.
26. Zhang P, Liegeois NJ, Wong C, Finegold M, Hou H, Thompson JC, et al. Altered cell differentiation and proliferation in mice lacking p57KIP2 indicates a role in Beckwith-Wiedemann syndrome. Nature. 1997;387:151–8.
27. Ito Y, Yoshida H, Nakano K, Kobayashi K, Yokozawa T, Hirai K, et al. Expression of p57/Kip2 protein in normal and neoplastic thyroid tissues. Int J Mol Med. 2002;9:373–6.
28. Ito Y, Yoshida H, Matsuzuka F, Matsuura N, Nakamura Y, Nakamine H, et al. Expression of the components of the Cip/Kip family in malignant lymphoma of the thyroid. Pathobiology. 2004;71:164–70.
29. Melck A, Masoudi H, Griffith OL, Rajput A, Wilkins G, Bugis S, et al. Cell cycle regulators show diagnostic and prognostic utility for differentiated thyroid cancer. Ann Surg Oncol. 2007;14:3403–11.
30. Higashimoto K, Soejima H, Saito T, Okumura K, Mukai T. Imprinting disruption of the CDKN1C/KCNQ1OT1 domain: the molecular mechanisms causing Beckwith-Wiedemann syndrome and cancer. Cytogenet Genome Res. 2006;113:306–12.
31. Kikuchi T, Toyota M, Itoh F, Suzuki H, Obata T, Yamamoto H, et al. Inactivation of p57KIP2 by regional promoter hypermethylation and histone deacetylation in human tumors. Oncogene. 2002;21:2741–9.
32. Kobatake T, Yano M, Toyooka S, Tsukuda K, Dote H, Kikuchi T, et al. Aberrant methylation of p57KIP2 gene in lung and breast cancers and malignant mesotheliomas. Oncol Rep. 2004;12:1087–92.
33. Lai S, Goepfert H, Gillenwater AM, Luna MA, El-Naggar AK. Loss of imprinting and genetic alterations of the cyclin-dependent kinase inhibitor p57KIP2 gene in head and neck squamous cell carcinoma. Clin Cancer Res. 2000;6:3172–6.

34. Borriello A, Caldarelli I, Bencivenga D, Criscuolo M, Cucciolla V, Tramontano A, et al. p57(Kip2) and cancer: time for a critical appraisal. Mol Cancer Res. 2011;9:1269–84.
35. Dauphinot L, De Oliveira C, Melot T, Sevenet N, Thomas V, Weissman BE, et al. Analysis of the expression of cell cycle regulators in Ewing cell lines: EWS-FLI-1 modulates p57KIP2and c-Myc expression. Oncogene. 2001;20:3258–65.
36. Mesbah K, Rana MS, Francou A, van Duijvenboden K, Papaioannou VE, Moorman AF, et al. Identification of a Tbx1/Tbx2/Tbx3 genetic pathway governing pharyngeal and arterial pole morphogenesis. Hum Mol Genet. 2012;21:1217–29.
37. Fagman H, Amendola E, Parrillo L, Zoppoli P, Marotta P, Scarfo M, et al. Gene expression profiling at early organogenesis reveals both common and diverse mechanisms in foregut patterning. Dev Biol. 2011;359:163–75.
38. Zhao L, Zevallos SE, Rizzoti K, Jeong Y, Lovell-Badge R, Epstein DJ. Disruption of SoxB1-dependent Sonic hedgehog expression in the hypothalamus causes septo-optic dysplasia. Dev Cell. 2012;22:585–96.